Calculation of the Ion Optical Properties of Inhomogeneous Magnetic Sector Fields, including the Second Order Aberrations in the Median Plane

By H. A. Tasman and A. J. H. Boerboom

Laboratorium voor Massaspectrografie, Amsterdam, Holland

(Z. Naturforschg. **14 a**, 121—129 [1959]; eingegangen am 3. September 1958)

Investigation is made of the ion optical properties of inhomogeneous magnetic sector fields. In first order approximation the field is assumed to vary proportional to r^{-n} $(0 \leqq n < 1)$; the term in the magnetic field expansion which determines the second order aberrations is chosen independent of n, which makes the elimination possible of e. g. the second order angular aberration. From the Euler–Lagrange equations the second order approximation of the ion trajectories in the median plane and the first order approximation outside the median plane are derived for the case of normal incidence and exit of the central path in the sector field. An equation is presented giving the shape of the pole faces required to produce the desired field. The influence of stray fields is neglected. The object and image distances are derived, as well as the mass dispersion, the angular, lateral and axial magnification, the resolving power, and the inclination of the plane of focus of the mass spectrum. The maximum transmitted angle in the z-direction is calculated. The resolving power proves to be proportional to $(1-n)^{-1}$ whereas the length of the central path is proportional to $(1-n)^{-1/2}$. An actual example is given of a 180° sector field with $n=0.91$, where the mass resolving power is increased by a factor 11 as compared with a homogeneous sector field of the same radius and slit widths.

The mass dispersion of magnetic analysers may be improved by employing an inhomogeneous magnetic field. A magnetic field which varies in the median plane proportional to $r^{-1/2}$ (Svartholm and Siegbahn [1]), as is used in many β-spectrometers, was chosen by Fischer [2] for a mass spectrometer; it offers the advantage of increased luminosity due to its two-directional focusing properties, whilst the mass dispersion and resolving power are increased by a factor 2 as compared with a homogeneous magnetic field analyser with the same radius of the central beam. Alekseevski et al. [3] pointed out, that both the mass dispersion and the resolution may be still further improved by the use of more inhomogeneous magnetic fields. By employing a magnetic field which varies in the median plane proportional to r^{-n} $(0 \leqq n < 1)$, the mass dispersion and resolution as compared with a homogeneous field $(n=0)$ increase proportional to $(1-n)^{-1}$, whilst the focusing angle increases proportional to $(1-n)^{-1/2}$. Choosing for example $n=0.91$, the resolving power is increased by a factor 11. However, the advantage of stigmatic focusing is lost for $n \neq 1/2$. The calculations of Alekseevski et al. apply to the paraxial rays only.

Calculations of the ion optical properties of general ψ-independent electromagnetic fields with circular central path have been published by Svartholm [4], Franke [5], and Grümm [6]. These authors assume both object and image to be situated within the field boundaries, and restrict their calculations of second order aberrations to stigmatic focusing fields, which correspond to $n=1/2$ for magnetic fields.

To obtain a very high resolving power, especially those fields are interesting in which n is close to unity. These fields must be of the sector type to be of physical significance. The present work was set up for finding expressions (for the median plane only) of the second order angular aberration (proportional to α^2), the second order velocity aberration (proportional to β^2), and the mixed second order aberration (proportional to $\alpha\beta$). The influence of stray fields is neglected; it is asumed that these fields can be compensated by suitable shields (Herzog [7, 8]), or taken into account as an effective field-length (König and Hintenberger [9]). For the present

[1] N. Svartholm and K. Siegbahn, Rev. Sci. Instrum. **19**, 594 [1948].
[2] D. Fischer, Z. Phys. **133**, 455; 471 [1952].
[3] N. E. Alekseevski et al., Dokl. Akad. Nauk SSSR **100**, 229 [1953].
[4] N. Svartholm, Ark. Fys. **2**, 20 [1950].
[5] H. W. Franke, Oest. Ing. Arch. **5**, 371 [1951]; **6**, 105 [1952].
[6] H. Grümm, Acta Phys. Austr. **8**, 119 [1953].
[7] R. Herzog, Z. Phys. **97**, 596 [1935].
[8] R. Herzog, Z. Naturforschg. **10 a**, 887 [1955].
[9] L. A. König and H. Hintenberger, Z. Naturforschg. **10 a**, 877 [1955].

the calculations are restricted to the case of straight field boundaries which are normal to the central beam at the point where it enters and leaves the field. The coefficient in the magnetic field expansion which determines the second order aberrations, is taken to be independent of the coefficient defining the paraxial rays. As inhomogeneous magnetic fields always require specially shaped pole faces, this degree of freedom seems to be easier to realize in practice than that of curved boundaries or that of oblique incidence or exit. The median plane is assumed to be a plane of symmetry.

1. Coordinate system

In the field free object and image space the rectilinear ion trajectories are expressed in cartesian coordinates x_1, y_1, z_1, and x_2, y_2, z_2, respectively. In the deflecting field region the main path is assumed to be circular with radius r_m, and the curved trajectories are expressed in the dimensionless coordinates: normal coordinate $u = (r - r_m)/r_m$ (in the plane of paper); binormal coordinate $v = z/r_m$ (perpendicular to the plane of paper); path coordinate $w = \psi$.

We will first calculate the ion trajectories in the magnetic field region, and then suppose the rectilinear paths in the field free object and image space to coincide with the tangents at the field boundaries.

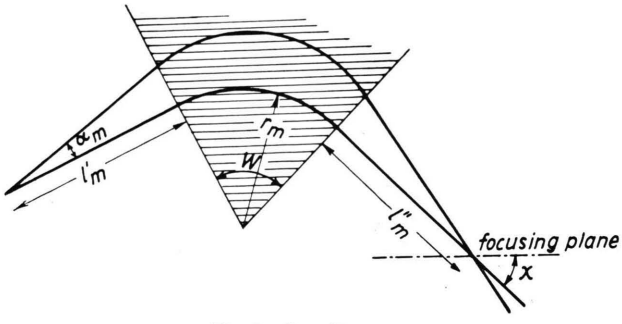

Fig. 1. Coordinate system.

2. The Euler–Lagrange equations

The ion trajectories are defined by the EULER-LAGRANGE equations: (GLASER [10, 11])

$$\frac{\mathrm{d}}{\mathrm{d}w}\left(\frac{\partial F}{\partial u'}\right) - \frac{\partial F}{\partial u} = 0\,, \tag{1}$$

$$\frac{\mathrm{d}}{\mathrm{d}w}\left(\frac{\partial F}{\partial v'}\right) - \frac{\partial F}{\partial v} = 0\,. \tag{2}$$

F is the ion optical "index of refraction", in this case given by

$$F(u, v, u', v') = \sqrt{(1+u)^2 + u'^2 + v'^2} - \sqrt{\frac{e}{2\,m\,U}}\,(1+u)\,A_w\,. \tag{3}$$

$u' = \mathrm{d}u/\mathrm{d}w$, and $v' = \mathrm{d}v/\mathrm{d}w$; the electrostatic potential U for ions of mass m and charge e should be taken zero at the point where the ions possess zero velocity. A_w is the w-component of the magnetic vector potential $\mathfrak{A}$.

We may expand F in a power series in u, v, u', and v'. This expansion contains no odd powers of u' or v', and the symmetry of A_w with respect to the median plane $v = 0$ causes terms with odd powers of v to vanish. F may be written in the form: (GRÜMM [6]) (up to terms of the third order included)

$$\begin{aligned} F(u, v, u', v') = {} & F_{00} + F_{10}\,u + F_{20}\,u^2 + F_{02}\,v^2 \\ & + \tfrac{1}{2}(u'^2 + v'^2) + F_{30}\,u^3 + F_{12}\,u\,v^2 \\ & - \tfrac{1}{2}\,u\,(u'^2 + v'^2) + \ldots\,. \end{aligned} \tag{4}$$

The coefficients F_{00}, F_{10}, etc. depend on

$$\eta = (e/2\,m\,U)^{1/2} = e/m\,v$$

of the ions and on the strength and shape of the magnetic field as expressed by A_w.

Successive approximations of the ion trajectories are found by substituting (4) into (1) and (2), retaining terms in (4) up to one order higher than that of the approximation wanted. The order of approximation is defined by the highest degree in u_0, α, v_0, γ, up to which all terms are included in the expression for the ion trajectories. u_0, α, v_0, and γ, are the values of u, u', v and v' respectively at $w = 0$ (boundary conditions); these quantities are assumed to be small of first order. The central path $u = v = 0$ should be a possible trajectory for ions of mass m_0, velocity v_0, and charge e_0. This corresponds to the zeroth order approximation, which may be expressed as the condition

$$F_{10}(e_0, m_0, v_0, A_w) = 0\,. \tag{5}$$

3. First order approximation of the ion trajectories

To get the first order approximation, terms up to the second order in (4) should be retained. Then from (4), (1), and (2) we find the two simul-

[10] W. GLASER, in: Handbuch der Physik (ed. S. FLÜGGE) **33**, p. 306 ff., Berlin 1956.
[11] W. GLASER, Z. Phys. **80**, 451 [1933].

taneous differential equations

$$u'' = 2 F_{20} u + F_{10}, \tag{6}$$

$$v'' = 2 F_{02} v \tag{7}$$

where $u'' = \mathrm{d}^2u/\mathrm{d}w^2$ and $v'' = \mathrm{d}^2v/\mathrm{d}w^2$.
If we write

$$k_1^2 = -2 F_{20}, \tag{8}$$

$$k_2^2 = -2 F_{02}, \tag{9}$$

the general solutions of (6) and (7) may be written in the form

$$u = a_1 \sin k_1 w + a_2 \cos k_1 w + F_{10}/k_1^2, \tag{10}$$

$$v = b_1 \sin k_2 w + b_2 \cos k_2 w. \tag{11}$$

If as boundary conditions are chosen the parameters defining the ion trajectory at $w = 0$

$$u(0) = u_0, \quad u'(0) = \alpha, \tag{12}$$

$$v(0) = v_0, \quad v'(0) = \gamma, \tag{13}$$

the particular solutions satisfying these boundary conditions are

$$u = {}^{(1)}u(w) = u_0 \cos k_1 w + \frac{\alpha}{k_1} \sin k_1 w + \frac{F_{10}}{k_1^2} (1 - \cos k_1 w), \tag{14}$$

$$v = {}^{(1)}v(w) = v_0 \cos k_2 w + \frac{\gamma}{k_2} \sin k_2 w. \tag{15}$$

4. Second order approximation of the ion trajectories in the median plane

In the median plane $v = v' = 0$, and we must only solve equation (1). Retaining terms up to the third order in (4), and substituting this expansion into (1) we find

$$u'' - 2 F_{20} u - F_{10} = 3 F_{30} u^2 + \tfrac{1}{2} u'^2 + u u''. \tag{16}$$

This equation can be solved by the method of variation of parameters if the right hand member can be written as a function of w, say $F(w)$. This can be accomplished by substituting the first order approximation (14), and the derivatives derived from it, into the right hand member of (16)

$$u'' - 2 F_{20} u - F_{10} = 3 F_{30} {}^{(1)}u^2 + \tfrac{1}{2} {}^{(1)}u'^2 + {}^{(1)}u \; {}^{(1)}u'' = F(w). \tag{17}$$

Then the second order approximation satisfying the boundary conditions (12) is given by

$$u = {}^{(2)}u(w) = {}^{(1)}u(w) + \frac{\sin k_1 w}{k_1} \int_0^w \cos k_1 w \, F(w) \, \mathrm{d}w - \frac{\cos k_1 w}{k_1} \int_0^w \sin k_1 w \, F(w) \, \mathrm{d}w. \tag{18}$$

Evaluation of $F(w)$ leads to

$$F(w) = C_1 \cos^2 k_1 w + C_2 \sin k_1 w \cos k_1 w + C_3 \sin^2 k_1 w + C_4 \cos k_1 w + C_5 \sin k_1 w + C_6, \tag{19}$$

where

$$C_1 = (3 F_{30} - k_1^2) u_0^2 + \tfrac{1}{2} \alpha^2 - 2 F_{10} k_1^{-2} (3 F_{30} - k_1^2) u_0 + F_{10}^2 k_1^{-4} (3 F_{30} - k_1^2),$$

$$C_2 = 3 k_1^{-1} (2 F_{30} - k_1^2) u_0 \alpha - 3 F_{10} k_1^{-3} (2 F_{30} - k_1^2) \alpha,$$

$$C_3 = \tfrac{1}{2} k_1^2 u_0^2 + k_1^{-2} (3 F_{30} - k_1^2) \alpha^2 - F_{10} u_0 + \tfrac{1}{2} k_1^{-2} F_{10}^2, \qquad C_5 = F_{10} k_1^{-3} (6 F_{30} - k_1^2) \alpha,$$

$$C_4 = F_{10} k_1^{-2} (6 F_{30} - k_1^2) u_0 - F_{10}^2 k_1^{-4} (6 F_{30} - k_1^2), \qquad C_6 = 3 F_{10}^2 k_1^{-4} F_{30}.$$

Straightforward integration leads to the second order approximation of the ion trajectories in the median plane:

$$u = {}^{(2)}u(w) = H_1 u_0 + H_2 \alpha + H_{11} u_0^2 + H_{12} u_0 \alpha + H_{22} \alpha^2 + H_3 \tag{20}$$

where

$$H_1 = \cos k_1 w - \tfrac{2}{3} F_{10} k_1^{-4} (3 F_{30} - k_1^2) (\sin^2 k_1 w - \cos k_1 w + 1) - \tfrac{1}{3} F_{10} k_1^{-2} (1 - \cos k_1 w)^2 + \tfrac{1}{2} F_{10} k_1^{-3} (6 F_{30} - k_1^2) w \sin k_1 w,$$

$$H_2 = k_1^{-1} \sin k_1 w + F_{10} k_1^{-5} (2 F_{30} - k_1^2) (\sin k_1 w \cos k_1 w - \sin k_1 w) + \tfrac{1}{3} F_{10} k_1^{-5} (6 F_{30} - k_1^2) (\sin k_1 w - k_1 w \cos k_1 w),$$

$$H_3 = F_{10} k_1^{-2} (1 - \cos k_1 w) + F_{10}^2 k_1^{-6} (F_{30} - \tfrac{1}{3} k_1^2) (\sin^2 k_1 w + 1 - \cos k_1 w) + \tfrac{1}{6} F_{10}^2 k_1^{-4} (1 - \cos k_1 w)^2 + 3 F_{10}^2 F_{30} k_1^{-6} (1 - \cos k_1 w) - \tfrac{1}{2} F_{10}^2 k_1^{-5} (6 F_{30} - k_1^2) w \sin k_1 w;$$

$H_{11} = \frac{1}{3} k_1^{-2} (3 F_{30} - k_1^2) (\sin^2 k_1 w + 1 - \cos k_1 w) + \frac{1}{6} (1 - \cos k_1 w)^2$,

$H_{12} = k_1^{-3} (2 F_{30} - k_1^2) (\sin k_1 w - \sin k_1 w \cos k_1 w)$,

$H_{22} = \frac{1}{6} k_1^{-2} (\sin^2 k_1 w + 1 - \cos k_1 w) + \frac{1}{3} k_1^{-4} (3 F_{30} - k_1^2) (1 - \cos k_1 w)^2$.

5. Correlation with the magnetic field shape

The coefficients F_{00}, F_{10}, F_{20}, F_{02}, F_{30}, and F_{12} should now be expressed in the magnetic field parameters and $(e/m\,v) = (e/2\,m\,U)^{1/2}$ of the ions. This may be done by expanding A_w in a power series:

$$A_w = \sum_{i,k} a_{ik}\, u^i\, v^k \tag{21}$$

and using the relations

$$\operatorname{div} \mathfrak{A} = 0\,, \qquad \nabla^2 A_w = 0 \tag{22}$$

(because $\mathfrak{A}$ can be chosen in such a way that A_w is the only component of $\mathfrak{A}$ differing from zero), and

$$B_u = -\,\partial A_w / \partial v\,, \tag{23}$$

$$B_v = \frac{1}{1+u} \frac{\partial}{\partial u} [(1+u)\, A_w]\,. \tag{24}$$

Writing instead of the coefficients a_{ik}, suitably chosen coefficients B, B_1, B_2, which express the relations between the coefficients a_{ik} derived from (22), (23), and (24), we may write for A_w, B_u, and B_v (see note [6])

$$A_w = \tfrac{1}{2} B + \tfrac{1}{2} B\, u + \tfrac{1}{2} B_1 (u^2 - v^2) - \tfrac{1}{3} (B_1 + B_2)\, u^3 + (\tfrac{1}{2} B_1 + B_2)\, u\, v^2 + \ldots, \tag{25}$$

$$B_u = B_1\, v - (B_1 + 2\,B_2)\, u\, v + \ldots, \tag{26}$$

$$B_v = B + B_1\, u - (\tfrac{1}{2} B_1 + B_2)\, u^2 + \mathrm{B}_2\, v^2 + \ldots. \tag{27}$$

For a magnetic field in which B_v in the median plane ($v = 0$) varies proportional to r^{-n}:

$$B_v(u, 0) = B(1+u)^{-n}, \tag{28}$$

the coefficients B_1 and B_2 are found by comparing (27) with the TAYLOR expansion of (28):

$$B_1/B = -n; \qquad B_2/B = -n^2/2\,. \tag{29}$$

However, we will assume the field shape to be given by (28) only in first order approximation. Then B_1/B is still given by

$$B_1/B = -n \tag{30}$$

but B_2/B is now independent of n, and may be written in the convenient form:

$$B_2/B = \tfrac{1}{2}\{X(1-n) - n\}\,. \tag{31}$$

The field shape defined by (30), (31) reduces to that given by (29) for $X \to n$.

From (3), (25), (30) and (31) we find for the coefficients in the expansion (4)

$$\left.\begin{aligned} F_{00} &= 1 - \tfrac{1}{2}\eta B\,, & F_{10} &= 1 - \eta B\,, \\ F_{20} &= -\tfrac{1}{2}(1-n)\,\eta B\,, & F_{02} &= -\tfrac{1}{2} n\,\eta B\,, \\ F_{30} &= \frac{X(1-n)}{6}\,\eta B\,, & F_{12} &= \frac{n - X(1-n)}{2}\,\eta B\,, \end{aligned}\right\} \tag{32}$$

where

$$\eta = e/m\,v = (e/2\,m\,U)^{1/2}\,. \tag{33}$$

If all ions are of charge e, but a momentum spread is allowed according to:

$$m\,v = m_0\, v_0 (1+\beta), \tag{34}$$

or

$$\eta = \eta_0/(1+\beta)\,, \tag{35}$$

the parameters η and B may be expressed in β, if we remind that from (5):

$$\eta_0 B = 1\,. \tag{36}$$

β is supposed to be a small quantity, small of first order. We may now substitute (32), (35) and (36) into (20), and then expand (20) in a TAYLOR series in β. Terms up to the second order included in u_0, α and β should be retained. Thus we find the following expression for the second order approximation of the ion trajectories in the median plane:

$$u = {}^{(2)}u(w) = D_1\, u_0 + D_2\, \alpha + D_3\, \beta + D_{11}\, u_0^2 + D_{12}\, u_0\, \alpha + D_{22}\, \alpha^2 + D_{13}\, u_0\, \beta + D_{23}\, \alpha\, \beta + D_{33}\, \beta^2\,, \tag{37}$$

where (with $w^* = (1-n)^{1/2} w$)

$$D_1 = \cos w^*, \qquad D_2 = (1-n)^{-1/2} \sin w^*, \qquad D_3 = (1-n)^{-1}(1 - \cos w^*)\,;$$

$D_{11} = \frac{1}{6}\{(X-3)\sin^2 w^* + X(1-\cos w^*)\}$,

$D_{12} = \frac{1}{3}(1-n)^{-1/2}(X-3)\sin w^*(1-\cos w^*)$,

$D_{22} = \frac{1}{6}(1-n)^{-1}\{(X-3)\cos^2 w^* - (2X-3)\cos w^* + X\}$,

$D_{13} = \frac{1}{6}(1-n)^{-1}\{-2(X-3)\sin^2 w^* - 2X(1-\cos w^*) + 3(X-n)\, w^* \sin w^*\}$,
$D_{23} = \frac{1}{6}(1-n)^{-3/2}\{2(X-3)\sin w^* \cos w^* + (X-3n+6)\sin w^* - 3(X-n)\, w^* \cos w^*\}$,
$D_{33} = \frac{1}{6}(1-n)^{-2}\{(X-3)\sin^2 w^* + 4X(1-\cos w^*) - 3(X-n)\, w^* \sin w^*\}$.

6. Imaging properties of the inhomogeneous magnetic sector field

To find the imaging properties of the sector field, we should calculate the tangents to the ion trajectory (37) at the point where it enters and leaves the field; these tangents are then supposed to coincide with the rectilinear paths in the field free object and image space. The object slit is assumed to be very narrow, and to lie on the central path at the object

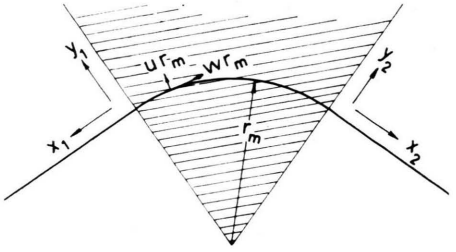

Fig. 2.

distance l_m'. From Fig. 2 it is obvious that (omitting terms of third and higher order),

$$u_0 = (l_m'/r_m)\,\alpha_m, \tag{38}$$

while

$$\alpha = (r/r_m)\,\alpha_m = (1+u_0)\,\alpha_m = \alpha_m + (l_m'/r_m)\,\alpha_m^2. \tag{39}$$

After passage through the sector field of sector angle W, the rectilinear path in the image space is given by

$$y_2 = r_m\, u(W) + (\mathrm{d}y_2/\mathrm{d}x_2)_{x_2=0}\, x_2. \tag{40}$$

Analogous to (39) we have the relation:

$$(\mathrm{d}y_2/\mathrm{d}x_2)_{x_2=0} = u'(W)\,[1-u(W)]. \tag{41}$$

From (37), (38), (39), (40), the ion path in the image space is given by

$$y_2 = r_m(M_1\,\alpha_m + M_2\,\beta + M_{11}\,\alpha_m^2 + M_{12}\,\alpha_m\,\beta + M_{22}\,\beta^2) + x_2(N_1\,\alpha_m + N_2\,\beta + N_{11}\,\alpha_m^2 + N_{12}\,\alpha_m\,\beta + N_{22}\,\beta^2),$$

where (42)

$$\left.\begin{aligned} M_1 &= \mu_{1a} + \mu_{1b}(l_m'/r_m), \qquad M_2 = \mu_{2a}, \\ M_{11} &= \mu_{11a} + \mu_{11b}(l_m'/r_m) + \mu_{11c}(l_m'/r_m)^2, \\ M_{12} &= \mu_{12a} + \mu_{12b}(l_m'/r_m), \qquad M_{22} = \mu_{22a}; \end{aligned}\right\} \tag{43}$$

$$\left.\begin{aligned} N_1 &= \nu_{1a} + \nu_{1b}(l_m'/r_m), \qquad N_2 = \nu_{2a}, \\ N_{11} &= \nu_{11a} + \nu_{11b}(l_m'/r_m) + \nu_{11c}(l_m'/r_m)^2, \\ N_{12} &= \nu_{12a} + \nu_{12b}(l_m'/r_m), \qquad N_{22} = \nu_{22a}. \end{aligned}\right\} \tag{44}$$

Expressions (42), (43) and (44) are valid for the median plane of *any* sector field in the arrangement of Fig. 2 (HINTENBERGER and KÖNIG [12–14]; KÖNIG and HINTENBERGER [15]).

For the particular magnetic field shape specified by (30), (31), or (32), (33), the coefficients μ_{1a}, etc., and ν_{1a}, etc. are given by (writing $W^* = (1-n)^{1/2} W$)

$$\mu_{1a} = (1-n)^{-1/2}\sin W^*, \qquad \mu_{1b} = \cos W^*, \qquad \mu_{2a} = (1-n)^{-1}(1-\cos W^*),$$
$$\mu_{11a} = \tfrac{1}{6}(1-n)^{-1}\{(X-3)\cos^2 W^* - (2X-3)\cos W^* + X\},$$
$$\mu_{11b} = \tfrac{1}{3}(1-n)^{-1/2}\{X\sin W^* - (X-3)\sin W^* \cos W^*\},$$
$$\mu_{11c} = \tfrac{1}{6}\{X(1-\cos W^*) + (X-3)\sin^2 W^*\}, \tag{45}$$
$$\mu_{12a} = \tfrac{1}{6}(1-n)^{-3/2}\{2(X-3)\sin W^* \cos W^* + (X-3n+6)\sin W^* - 3(X-n)\, W^* \cos W^*\},$$
$$\mu_{12b} = \tfrac{1}{6}(1-n)^{-1}\{-2(X-3)\sin^2 W^* - 2X(1-\cos W^*) + 3(X-n)\, W^* \sin W^*\},$$
$$\mu_{22a} = \tfrac{1}{6}(1-n)^{-2}\{(X-3)\sin^2 W^* + 4X(1-\cos W^*) - 3(X-n)\, W^* \sin W^*\}.$$

$$\nu_{1a} = \cos W^*, \qquad \nu_{1b} = -(1-n)^{1/2}\sin W^*, \qquad \nu_{2a} = (1-n)^{-1/2}\sin W^*,$$
$$\nu_{11a} = \tfrac{1}{6}(1-n)^{-1/2}\{-2X\sin W^* \cos W^* + (2X-3)\sin W^*\},$$

[12] H. HINTENBERGER and L. A. KÖNIG, Z. Naturforschg. **11 a**, 1039 [1956].
[13] H. HINTENBERGER and L. A. KÖNIG, Z. Naturforschg. **12 a**, 140 [1957].
[14] H. HINTENBERGER and L. A. KÖNIG, Z. Naturforschg. **12 a**, 773 [1957].
[15] L. A. KÖNIG and H. HINTENBERGER, Z. Naturforschg. **12 a**, 377 [1957].

$$
\begin{aligned}
\nu_{11b} &= \tfrac{1}{3} X \{2 \sin^2 W^* + \cos W^* - 1\}, \\
\nu_{11c} &= \tfrac{1}{6} (1-n)^{1/2} X \{2 \sin W^* \cos W^* + \sin W^*\}, \\
\nu_{12a} &= \tfrac{1}{6} (1-n)^{-1} \{-4 X \sin^2 W^* + 2 X (1 - \cos W^*) + 3 (X-n) W^* \sin W^*\}, \\
\nu_{12b} &= \tfrac{1}{6} (1-n)^{-1/2} \{-4 X \sin W^* \cos W^* + (X - 3n + 6) \sin W^* + 3 (X-n) W^* \cos W^*\}. \\
\nu_{22a} &= \tfrac{1}{6} (1-n)^{-3/2} \{2 X \sin W^* \cos W^* + (X + 3n - 6) \sin W^* - 3 (X-n) W^* \cos W^*\}.
\end{aligned}
\tag{46}
$$

For very small values of β, the term proportional to α_m in (42) vanishes for $x_2 = -r_m(M_1/N_1)$. This means that first order direction focusing occurs at the image distance

$$l_m'' = -r_m(M_1/N_1). \tag{47}$$

(47) may be written in the familiar form:

$$(l_m'' - g'')(l_m' - g') = f^2, \tag{48}$$

where f is the focal length, and g'' and g' are respectively the image and object distances corresponding to $l_m' = \infty$ or $l_m'' = \infty$. For the particular magnetic field shape expressed by (30), (31), these quantities are equal to

$$f = r_m (1-n)^{-1/2} \operatorname{cosec} W^*, \tag{49}$$

$$g' = g'' = g = r_m (1-n)^{-1/2} \cot W^*. \tag{50}$$

If all ions are of energy eU, but a small difference in mass is allowed according to

$$m = m_0 + \delta m, \tag{51}$$

the corresponding value of β is given in first order by

$$\beta = \delta m / 2 m_0. \tag{52}$$

The mass dispersion in the y_2-direction at the image distance l_m'', per unit $\delta m/m_0$ for a mono-energetic ion beam is given by

$$D_m = \tfrac{1}{2} r_m [M_2 - (M_1/N_1) N_2]. \tag{53}$$

However, the focusing plane of the mass spectrum need not be perpendicular to the central path, as the image distance depends on the mass difference according to

$$l_m'' = -r_m \frac{M_1 + \frac{1}{2} M_{12} (\delta m/m_0)}{N_1 + \frac{1}{2} N_{12} (\delta m/m_0)}. \tag{54}$$

If all ions have the same momentum ($\beta = 0$), the image width of an infinitely narrow object slit is limited by the second order angular aberration:

$$A_{11} \alpha_m^2 = r_m [M_{11} - (M_1/N_1) N_{11}] \alpha_m^2. \tag{55}$$

Object and image are at the same electrostatic potential; thus the lateral magnification M_{lat} is the reciprocal of the angular magnification M_{ang}. Omitting second order terms in y_2, we have

$$M_{ang} = \partial (\mathrm{d}y_2/\mathrm{d}x_2)/\partial \alpha_m = N_1, \tag{56}$$

and consequently

$$M_{lat} = 1/N_1. \tag{57}$$

The same result is found (as it should) if the axial magnification M_{ax} is derived from (48):

$$M_{ax} = \partial l_m''/\partial l_m' = -(l_m'' - g)/(l_m' - g), \tag{58}$$

and the relation

$$M_{lat} = -M_{ang} \cdot M_{ax} \tag{59}$$

is used.

If the sector field is used for a mass spectrometer, the mass resolving power (the reciprocal of the relative mass difference $\delta m/m_0$ which will just be resolved) is given by

$$R = D_m/(s' M_{lat} + s'' + \Sigma A_i) \tag{60}$$

where s' and s'' are the object and image slit widths respectively, and ΣA_i stands for the total image broadening due to all aberrations. If there is no energy spread in the ion beam, if the image slit is placed at the correct image distance l_m'', and if third and higher order aberrations may be neglected, the mass resolving power in the median plane is given by

$$R = D_m/(s' M_{lat} + s'' + A_{11} \alpha_m^2). \tag{61}$$

7. Transmission of ions outside the median plane

The trajectory of ions emerging from the centre of the object slit ($y_1 = z_1 = 0$; $x_1 = l_m'$) with a velocity component normal to the median plane equal to $-\mathrm{d}z_1/\mathrm{d}x_1 = \gamma_m$, may be found in first order approximation by substituting

$$v_0 = (l_m'/r_m)\, \gamma_m; \quad \gamma = \gamma_m, \tag{62}$$

into (15). With (32), and using a procedure analogous to that for derivation of (37) but retaining only first order terms, we find for the trajectory within the sector field (with $w^\dagger = n^{1/2} w$)

$$v = \gamma_m (n^{-1/2} \sin w^\dagger + (l_m'/r_m) \cos w^\dagger). \quad (63)$$

In the image space the trajectory is given by (with $W^\dagger = n^{1/2} W$)

$$z_2 = \gamma_m \{r_m (n^{-1/2} \sin W^\dagger + (l_m'/r_m) \cos W^\dagger) + x_2 (\cos W^\dagger - n^{1/2} (l_m'/r_m) \sin W^\dagger)\}. \quad (64)$$

The maximum value of $|\gamma_m|$ which can pass through the image slit is limited either by the width of the analyser tube within the sector field (extending from $v = -D/2$ to $v = +D/2$), or by the height of the image slit (extending from $z_2 = -h''/2$ to $z_2 = +h''/2$). From (63) we find by differentiation that

$$|v| = |v|_{max} \quad \text{for} \quad \cot w^\dagger = n^{1/2} (l_m'/r_m). \quad (65)$$

The maximum value of $|\gamma_m|$ which can pass through the analyser tube is given by:

$$|\gamma_m|_{max} = \frac{1}{2} \sqrt{\frac{D^2 n}{1 + n (l_m'/r_m)^2}} \quad (66)$$

if $\cot W^\dagger \leq n^{1/2} l_m'/r_m$,

or by

$$|\gamma_m|_{max} = \frac{1}{2} \frac{D n^{1/2}}{\sin W^\dagger + n^{1/2} (l_m'/r_m) \cos W^\dagger} \quad (67)$$

if $\cot W^\dagger \geq n^{1/2} l_m'/r_m$.

In the image space the ions seem to come, as regarding the z_2 component of their position and velocity, from a usually virtual object, separated from the image slit by the distance l_z, which is given by

$$l_z = l_m'' + r_m n^{-1/2} \frac{\sin W^\dagger + n^{1/2} (l_m'/r_m) \cos W^\dagger}{\cos W^\dagger - n^{1/2} (l_m'/r_m) \sin W^\dagger} \quad (68)$$

whereas the angular magnification in the z direction M^z_{ang} equals

$$M^z_{ang} = \cos W^\dagger - n^{1/2} (l_m'/r_m) \sin W^\dagger. \quad (69)$$

The maximum value of $|\gamma_m|$ which is determined by the image slit height is given by

$$|\gamma_m|_{max} = \frac{1}{2} \frac{h''}{l_z M^z_{ang}} = \frac{1}{2} \frac{n^{1/2} r_m h''}{(r_m^2 - n l_m' l_m'') \sin W^\dagger + n^{1/2} r_m (l_m' + l_m'') \cos W^\dagger}. \quad (70)$$

The actual value of $|\gamma_m|_{max}$ is set by either (66) and (67), or by (70), whichever is the smaller of the two.

In the homogeneous magnetic sector field there is no focusing action in the z direction (except through stray fields which are neglected in this paper), and thus the limit on $|\gamma_m|_{max}$ is determined by the image slit height:

$$|\gamma_m|_{max} = \frac{1}{2} \frac{h''}{l_m' + l_m'' + W r_m} \quad (71)$$

or by

$$|\gamma_m|_{max} = \frac{1}{2} \frac{D r_m}{l_m' + W r_m} \quad (72)$$

whichever is the smaller one.

(71), (72), serve for comparison with homogeneous sector fields. Whether or not a lower value of $|\gamma_m|_{max}$ results in a serious loss in transmission depends on the angular intensity distribution of the ion beam emerging from the object slit, and thus on the ion source design.

8. Shape of the pole faces

If the pole shoe material has a sufficiently high permeability at the field strength used, its surface is a surface of constant scalar magnetic potential φ_m. As the magnetic field strength $\mathfrak{B}$ equals:

$$\mathfrak{B} = -\operatorname{grad} \varphi_m, \quad (73)$$

the scalar magnetic potential corresponding to (21), (22), (23), (24), (26), (27), (30), and (31), may be written in the form (including terms up to the fifth order):

$$\varphi_m = B[-v + n u v + \tfrac{1}{2}\{X(1-n) - 2n\} u^2 v - \tfrac{1}{6}\{X(1-n) - n\} v^3 - C_3 u^3 v + \{\tfrac{1}{2}n - \tfrac{1}{6}X(1-n) + C_3\} u v^3 - C_4 u^4 v + \{-\tfrac{1}{2}n + \tfrac{1}{6}X(1-n) + \tfrac{1}{2}C_3 + 2C_4\} u^2 v^3 + \{\tfrac{1}{40}n - \tfrac{1}{120}X(1-n) - \tfrac{1}{10}C_3 - \tfrac{1}{5}C_4\} v^5 + \ldots]. \quad (74)$$

The so far undetermined coefficients C_3 and C_4 define the fourth and fifth order contributions to the field shape.

To calculate the shape of the pole faces required to produce a magnetic field with given values of n and X, the gap width at radius r_m should be given. Substitution of the corresponding value of v, and $u = 0$, into (74) gives the value of φ_m/B, which should be a constant for the surface of the pole face. There is an infinite number of profiles satisfying this condition, differing only in the contribution of fourth and higher order terms. If we put $C_3 = C_4 = 0$ and neglect terms of sixth and higher order, there is an unique solution which is best found by an

iterative process. Starting from $u=0$, an approximate value of v for some value of $u \neq 0$ is found using the slope dv/du along the profile, which equals

$$\left(\frac{dv}{du}\right)_{\varphi_m = \text{const}} = -\left(\frac{\partial \varphi_m}{\partial u}\right) \Big/ \left(\frac{\partial \varphi_m}{\partial v}\right). \quad (75)$$

This value is substituted only in the v^3-, $u\,v^3$-, $u^2\,v^3$-, and v^5-terms in (74), and a better approximation is found, which may be substituted again in the v^3-term etc., to give a third approximation, and so on. The process converges quickly in most practical cases, because v is usually much smaller than unity.

9. Symmetric arrangement

If in addition to the symmetry with respect to the median plane, the arrangement is also symmetric with respect to the plane $w = W/2$, some expressions become particularly simple. This extra condition of symmetry is satisfied or nearly satisfied in most existing mass spectrometers.

Now $l_m'' = l_m' = l_m$, and $M_{ang} = M_{lat} = M_{ax} = -1$.

From (56) we deduce

$$l_m/r_m = (1-n)^{-1/2} \cot(W^*/2). \quad (76)$$

The mass dispersion of a monoenergetic ion beam per unit $\delta m/m_0$ reduces from (53) to

$$D_m = (1-n)^{-1} r_m. \quad (77)$$

The coefficient of the second order angular aberration reduces from (55) to

$$A_{11} = \frac{r_m}{1-n}\left[X \frac{\cos W^* + 5}{3(1-\cos W^*)} - 1\right]. \quad (78)$$

Thus the second order angular aberration vanishes for

$$X = \frac{3(1-\cos W^*)}{\cos W^* + 5}. \quad (79)$$

10. An actual numerical example

To avoid unduly large object and image distances, the sector angle for an inhomogeneous field mass spectrometer should not be made too small. Therefore we choose $W = \pi$. Suppose $n = 0.91$, or $W^* = 0.3\,\pi = 54°$. If we restrict the discussion to the symmetric arrangement in the sense of sect. 9, (76) gives the object and image distance: $l_m = 6.542\, r_m$. According to (79), the second order angular aberration in the median plane vanishes for $X = +0.22131$. However, outside the median plane second order geometrical aberrations still exist (BOERBOOM[16]). If we neglect these, and also third and higher order aberrations, and if we assume: $r_m = 200$ mm, and $s' = s'' = 0.1$ mm, the mass resolving power in the absence of energy spread equals: $R = 11\,000$. To obtain this resolving power, the relative velocity spread should be much smaller than 1/11 000. This condition can only be satisfied by sufficient accelerating voltage, and special ion source design (DUBROVIN et al.[17]), and for ions not resulting from a dissociation of a two-atomic molecule (MORRISON and STANTON[18]). Otherwise a double focusing arrangement will be required, the design of which will be the subject of a subsequent paper. From (54), the mass dependence of the image distance is represented by

$$l_m''/r_m = 6.542 + 18.500\ (\delta m/m_0).$$

With (77), we can find the angle between the focusing plane of the mass spectrum and the central path $\chi = 31°\,0'$. The present calculations do not allow a prediction of the shape of the focusing plane. To find the curvature near the central path, we should retain the terms proportional to $\alpha_m \beta^2$ in (42); the position of a more extended range of the mass spectrum is determined by terms containing higher powers of β. The coefficients of these terms may be found by retaining terms of higher order in β in the TAYLOR expansion (37).

The shape of the pole shoes required to create the field with $n = 0.91$ and $X = 0.22131$, assuming infinite permeability of the pole shoe material, is given in the table below, where the effect of the finite extension in the radial direction is neglected. The z-coordinate (in mm) measured from the median plane is given for a number of values of the radius r (in mm) for three gap widths at radius $r_m = 200$ mm: a) gap width = 20.000 mm; b) gap width = 8.000 mm; c) gap width = 4.000 mm.

r(mm)	z(mm)			r(mm)	z(mm)		
	a)	b)	c)		a)	b)	c)
100	5.950	2.381	1.190	200	10.000	4.000	2.000
110	6.279	2.513	1.256	204	10.182	4.073	2.036
120	6.628	2.652	1.326	208	10.363	4.145	2.073
130	6.996	2.800	1.400	212	10.543	4.217	2.108
140	7.382	2.954	1.477	216	10.721	4.287	2.144
150	7.787	3.116	1.558	220	10.896	4.357	2.179
160	8.207	3.284	1.642	230	11.319	4.527	2.263
170	8.643	3.458	1.729	240	11.716	4.684	2.342
180	9.089	3.636	1.818	250	12.074	4.827	2.413
184	9.270	3.709	1.854	260	12.385	4.951	2.475
188	9.452	3.781	1.891	270	12.642	5.053	2.526
192	9.635	3.854	1.927	280	12.832	5.129	2.564
196	9.817	3.927	1.964	290	12.954	5.177	2.588
200	10.000	4.000	2.000	300	13.001	5.196	2.597

Tab. 1. Shape of the pole shoes for $n = 0.91$ and $X = 0.22131$.

From (66) we calculate $|\gamma_m|_{max} = 0.0755\, D$, whereas (70) gives $|\gamma_m|_{max} = 0.0268\, h''/r_m$. Thus the

[16] A. J. H. BOERBOOM, Appl. Sci. Res. **B 7**, 52 [1958].
[17] A. V. DUBROVIN et al., Dokl. Akad. Nauk SSSR **102**, 719 [1955].
[18] J.D.MORRISON and H.E.STANTON, J. Chem. Phys. **28**, 9 [1958].

image slit height will limit $|\gamma_m|$ if the width of the analyser tube within the sector field exceeds $0.355\,h''$; this will usually be the case. If we assume $h''=15$ mm, or $h''/r_m=0.075$, then $|\gamma_m|_{max}=0.00201$ rad.

A homogeneous sector field of 54° sector angle in a symmetric arrangement in the sense of sect. 9, would require $l_m'=l_m''=r_m \cot 27°=1.9626\,r_m$. With the same values $r_m=200$ mm, and $s'=s''=0.1$ mm, the maximum resolving power in the absence of energy spread equals $R=1000$. Now the second order angular aberration in the median plane is not zero; the coefficient A_{11} equals $-r_m$, and a beam divergence at the object slit of $\alpha_m=0.01$ rad. causes an image broadening of 0.02 mm which reduces the resolving power to about 800. If $|\gamma_m|$ is limited by the image slit height, $h''/r_m=0.075$ corresponds to $|\gamma_m|_{max}=0.00769$ rad. Whether the lower value of $|\gamma_m|_{max}$ for the inhomogeneous field as compared with the 54° homogeneous sector field, results in a serious loss in luminosity or not, depends on the angular spread of the beam emerging from the ion source, and thus on the ion source design.

Because the central path is longer with the inhomogeneous field than it is with the homogeneous field, the vacuum requirements for an inhomogeneous field mass spectrometer are more rigid. To obtain the same peak broadening due to the residual gas, the pressure in the analyser tube of the inhomogeneous field instrument discussed above, should be at least three times lower than in the 54° homogeneous sector field instrument. To make full use of the high resolving power of the inhomogeneous field, a pressure as much as 30 times lower than the maximum for the homogeneous field may be required, unless one reduces the collision cross sections, e. g. by increasing the accelerating voltage of the ions.

Acknowledgement

The authors wish to thank Prof. Dr. J. KISTEMAKER for his stimulating interest, and Drs. J. Los for his valuable criticism on the manuscript.

This work is part of the program of research of the Stichting voor Fundamenteel Onderzoek der Materie, and was made possible by financial support of the Nederlandse Organisatie voor Zuiver Wetenschappelijk Onderzoek.

Berechnung eines doppelfokussierenden stigmatisch abbildenden Massenspektrographen

Von H. EWALD, H. LIEBL und G. SAUERMANN

Aus dem Physikalischen Institut der Technischen Hochschule München

(Z. Naturforschg. **14 a**, 129—137 [1959]; eingegangen am 11. Oktober 1958)

In der vorliegenden Arbeit werden die Berechnungsunterlagen für einen praktisch ausgeführten [1], mit Toroidkondensator ausgerüsteten und stigmatisch abbildenden doppelfokussierenden Massenspektrographen zusammengestellt. Bei diesem Apparat wird der durch den relativ großen axialen Öffnungswinkel α_z bewirkte radiale Bildfehler f_{33} durch eine entsprechend berechnete Zylinderkrümmung der Austrittsstirnfläche des Toroidkondensators korrigiert.

Die bisher zu Präzisionsmessungen von Isotopenmassen verwendeten doppelfokussierenden Massenspektrographen haben Fokussierung nur in radialer Richtung *, d. h. nur in der Richtung der mittleren Umlenkebene. Senkrecht zu dieser Ebene, d. h. in der Richtung der Massenlinien (in axialer Richtung) laufen die Ionen auf ihren Wegen durch die Apparaturen unbeeinflußt im Bereich der von den Ionenquellen ausgeleuchteten Divergenzwinkel auseinander (etwa 1 Grad). Dies ist auf die Verwendung von homogenen Magnetfeldern und Zylinderkondensatoren zurückzuführen, die die Eigenschaften von Zylinderlinsen haben. Aus diesem Grunde werden die von den Ionenquellen gelieferten Intensitäten auf unnötig lange Massenlinien verteilt. Zu erheblichen Anteilen werden sie meist sogar durch die Backen von im Strahlengang befindlichen, in axialer Richtung wirksamen Apertur-Blenden abgefangen. Als solche Apertur-Blenden können z. B. vor dem Magnetfeld angebrachte Blenden fungieren, die zugleich als Streufeldabschirmung dienen.

Wie früher [2] gezeigt worden ist, muß bei genauen Isotopenmassen-Bestimmungen ein sehr kurzer Spalt verwendet werden (Länge etwa 0,2 mm), so daß die Länge der Massenlinien dann etwa 10 – 50-mal grö-

[1] G. SAUERMANN u. H. EWALD, Z. Naturforschg. **14 a**, 137 [1959].

* Radialschnitt ist in der Optik Hauptschnitt des Prismas.

[2] H. EWALD, Z. Naturforschg. **3 a**, 115 [1948].